UC Davis
UC Davis Previously Published Works

Title
Characterization of decavanadate and decaniobate solutions by Raman spectroscopy

Permalink
https://escholarship.org/uc/item/2s6290t0

Journal
Dalton Transactions, 45(17)

ISSN
1477-9226

Authors
Aureliano, Manuel
Ohlin, C André
Vieira, Michele O
et al.

Publication Date
2016-04-25

DOI
10.1039/c5dt04176g

Peer reviewed

PAPER

Characterization of decavanadate and decaniobate solutions by Raman spectroscopy†

Manuel Aureliano,*[a,b] C. André Ohlin,[c] Michele O. Vieira,[b] M. Paula M. Marques,[b,d] William H. Casey[e] and Luís A. E. Batista de Carvalho[b]

The decaniobate ion, (Nb_{10} = $[Nb_{10}O_{28}]^{6-}$) being isoelectronic and isostructural with the decavanadate ion (V_{10} = $[V_{10}O_{28}]^{6-}$), but chemically and electrochemically more inert, has been useful in advancing the understanding of V_{10} toxicology and pharmacological activities. In the present study, the solution chemistry of Nb_{10} and V_{10} between pH 4 and 12 is studied by Raman spectroscopy. The Raman spectra of V_{10} show that this vanadate species dominates up to pH 6.45 whereas it remains detectable until pH 8.59, which is an important range for biochemistry. Similarly, Nb_{10} is present between pH 5.49 and 9.90 and this species remains detectable in solution up to pH 10.80. V_{10} dissociates at most pH values into smaller tetrahedral vanadate oligomers such as V_1 and V_2, whereas Nb_{10} dissociates into Nb_6 under mildly (10 > pH > 7.6) or highly alkaline conditions. Solutions of V_{10} and Nb_{10} are both kinetically stable under basic pH conditions for at least two weeks and at moderate temperature. The Raman method provides a means of establishing speciation in the difficult niobate system and these findings have important consequences for toxicology activities and pharmacological applications of vanadate and niobate polyoxometalates.

1. Introduction

Decavanadate ($[V_{10}O_{28}^{6-}]$, V_{10}) is a member of a larger family of Group V and VI polyoxoanions commonly known as polyoxometalates (POMs). POMs have been found to have anti-diabetic, -bacterial, -protozoal, -viral and -cancer activities, which have sparked interest in their use as bio-inorganic drugs.[1–4] Decavanadate is a homoleptic isopolyoxovanadate that interacts with high affinity with several proteins such as myosin, actin, and Ca^{2+}-ATPase, thus affecting a range of cellular processes, including calcium homeostasis, muscle contraction, cytoskeleton dynamics and mitochondrial oxygen consumption.[4–11] Furthermore, the antidiabetic, anti-virus, anti-bacterial and anti-tumor activities of V_{10} and vanadate compounds are attracting increasing interest.[12–18] Decavanadate also exhibits insulin-mimetic behavior, and it was shown that, upon incubation with decavanadate, rat adipocytes accumulate much more glucose than with well-established mimetic agents such as BMOV.[18] Decavanadate is in many

cases likely a pro-drug, inducing anti-diabetic activity through peroxovanadate production.[17] On the other hand, *in vivo* exposure to decavanadate, in comparison with vanadate, affects differently subcellular metal distribution, antioxidant enzyme activities, lipid peroxidation and tissue damage in several organs.[4,9,10,19] Recently, decavanadate has also found application in other processes such as aerobic oxidation of starch, solar-driven photocatalysis and protein crystallography.[20–22]

Depending on factors such as vanadate concentration, pH and ionic strength, different vanadate oligomeric species can occur simultaneously in vanadium(V) solutions, including monomeric (V_1, $[VO_4]^{3-}$ at high pH), dimeric (V_2, $[V_2O_7]^{4-}$), tetrameric (V_4, $[V_4O_{12}]^{4-}$ and $[V_4O_{13}]^{6-}$), and pentameric (V_5, $[V_5O_{15}]^{5-}$) vanadates.[4,23,24] These ortho and metavanadate species are comprised of tetrahedral vanadate units. In addition to them, the decavanadate ion, V_{10}, which consists of octahedral vanadate units, also occurs in solution. Its presence is easily detected due to the strong orange-yellow colour of V_{10} compared with the colourless ortho and metavanadates.

Whereas an equilibrium between the ortho and metavanadate species is achieved on the millisecond-to-second time scale in neutral and alkaline aqueous solutions, V_{10} interconversion with the other vanadate oligomers occurs on a considerably longer time scale. The disappearance of the decamer follows a first-order kinetic process and can be easily followed by UV/Vis spectroscopy by recording the absorption band at 400 nm as a function of time.[4–6] In addition, V_{10} decompo-

[a] *FCT and CCmar, University of Algarve, 8005-139 Faro, Portugal.*
E-mail: maalves@ualg.pt; Fax: +351 289 800066; Tel: +351 289 800905
[b] *Unidade de I&D Química-Física Molecular, Department of Chemistry, University of Coimbra, Portugal*
[c] *School of Chemistry, Monash University, Clayton, Vic 3800, Australia*
[d] *Department of Life Sciences, University of Coimbra, 3004-535 Coimbra, Portugal*
[e] *Department of Chemistry, University of California, Davis, California 95616, USA*
† Electronic supplementary information (ESI) available. See DOI: 10.1039/c5dt04176g

sition may be prevented through binding to specific proteins, which apparently retard dissociation. Increases in the half-life from 5 to 17 hours in the presence of sarcoplasmic reticulum vesicles, and to 27 hours in the presence of actin were found at room temperature and pH 7.0,[25] whereas no effects were observed with myosin, even though it is known to have a high-affinity V_{10}-binding site.[26]

Decavanadate was observed to induce protein cysteine oxidation and vanadyl formation in the presence of SR Ca^{2+}-ATPase and actin, whereas no effects were observed on incubation with monomeric vanadate.[7,10,27] This reactivity of V_{10} was attributed to the involvement of cysteines at the V_{10}-binding site, as well as the participation of reduced vanadyl (V^{IV}-containing) species in the enzymatic inhibition process.[10] It is known that actin, in common with other proteins such as transferrin and albumin, contains a high affinity binding site for vanadyl.[7] Decavanadate interactions with certain proteins can thus lead to vanadyl protein binding, although the participation of vanadyl in the process is yet to be clarified.[10]

Other mono- and polyoxometalates, such as niobates, tungstates and molybdates, have also been evaluated in the inhibition of SR calcium ATPase and were found to be less active as inhibitors.[28] The decavanadate, V_{10}, and decaniobate (Nb_{10} = $[Nb_{10}O_{28}]^{6-}$) ions are isostructural and isovalent, but where vanadium is redox active and labile in solution, niobium is kinetically inert and redox stable, making Nb_{10} an excellent tool to explore the mode of inhibition that the V_{10} analogue undergoes with the proteins.[27,28]

The Nb_{10} and V_{10} compounds differ in their sizes, their ability to dissociate, their acid–base chemistry and their dissociation products. For example, there are no equivalents to the oligomeric metavanadates for niobium, which dissociates to the hexaniobate Lindqvist ion (Nb_6 = $[Nb_6O_{19}]^{8-}$) and derivatives. In spite of these differences the decaniobate ion can be a useful tool to understand the mechanism and biological activities of the decavanadate ion because of the structural similarity and relatively inert behaviour.[27,28]

Raman spectroscopy has been shown to be a suitable tool for investigating vanadate speciation, including oligomerization and its dependence on concentration, ionic strength and pH,[29] as well as decavanadate interactions with different Ca^{2+}-ATPase conformations.[27] We presently use Raman spectroscopy to further characterize aqueous solutions of decavanadate and decaniobate in order to determine differences in the ensemble of oligomeric species present under experimental conditions, which may be important in biochemical studies where the two families of ions are compared.[27,28] The application of vibrational spectroscopy to niobate solutions is particularly important because, although the predominant Nb nucleus is NMR active (^{93}Nb; $I = 9/2$), it yields broad lines in solution because of quadrupolar broadening. In contrast, vanadium NMR ^{51}V; $I = 7/2$) yields relatively narrow lines as it is less affected by quadrupolar broadening. Niobate speciation can only be practically monitored by NMR by enriching the compounds with ^{17}O and watching the ^{17}O NMR signal area change with time, but this is inherently limited[30] and expensive.

In contrast with vanadate, there is less precedence for Raman spectroscopy on niobate solutions. Apart from a few examples of Raman spectra of the $[Nb_6O_{19}]^{8-}$ ion at static pH[31,32] early pH-dependent work was carried out prior to the isolation of Nb_{10}, leading researchers then[33] and later[34] to assign the signals of this ion to a dodecameric species, which required later revision. In addition, a tetrameric niobate was reported by Spinner et al.[33] but this putative oligomer has never been isolated. There is thus a need for spectroscopic Raman data of niobate species to correct the existing literature.

2. Materials and methods

All reagents were of biochemical analysis grade and were supplied by BDH, Merck, and Sigma. Anhydrous ammonium metavanadate was purchased from Riedel-de Haën. Tetramethylammonium decaniobate, $[N(CH_3)_4]_6[Nb_{10}O_{28}]\cdot6H_2O$, was synthesised according to published procedures.[35] The synthesis of $K_7H[Nb_6O_{19}]$ was via adaptation of a standard method.[36]

2.1 Preparation of solutions

Decavanadate stock solution was prepared in MilliQ water (conductivity <0.055 µS cm^{-1} at 25 °C), by adjusting the pH of an ammonium metavanadate solution (50 mM, pH 6.7) to 4.0, according to literature methods,[26,27] and the formation of the V_{10} ion was readily observed by the characteristic orange-yellow colour of the solution.[4] Thus, we obtained a stock decavanadate concentration of 5 mM V_{10} (i.e. 50 mM total vanadium, ~50 mM NH_4^+). A solution of Nb_{10} was prepared in water as a stock concentration of 5 mM (i.e. 50 mM of niobium) by dissolving the tetramethylammonium salt. pH meter calibration was performed before each measurement with three standards from Hanna (4.01, 7.01 and 10.01). The solutions were prepared in MilliQ water (conductivity <0.055 µS cm^{-1} at 25 °C). The pH was adjusted by the addition of 0.1 M of HCl or 0.1 M NaOH.

2.2 NMR spectroscopy

^{51}V NMR spectroscopy measurements of V_{10} and vanadate stock solutions were performed on a Bruker AM-400 MHz (9.4 T; ^{51}V 105.2 MHz) spectrometer equipped with a 5 mm multinuclear inverse probe. The spectra were acquired at 22 °C using 0.5 mL of samples containing 10% D_2O using a calibrated π/2 pulse. 12 000–25 000 scans were acquired with recycling delays of 10 ms and acquisition times of 86 ms at a spectral width of 45.454 kHz. The ^{51}V NMR chemical shifts are reported relative to an external reference of $VOCl_3$, as described in previous work.[28]

2.3 High resolution Raman spectroscopy

The Raman spectra were recorded at room temperature, in a triple monochromator HORIBA Jobin-Yvon T64000 Raman system (focal distance 0.64 m, aperture f/7.5), equipped with

holographic gratings of 1800 grooves per mm. The premonochromator stage was used in the subtractive mode. The detection system was a liquid-nitrogen-cooled non-intensified 1024 × 256 pixel (1″) Charge Coupled Device (CCD) chip. A 90° geometry between the incident radiation and the collecting system was employed. The entrance slit was set to 200 μm, while the slit between the premonochromator and the spectrograph was set to 3.5×10^4 μm. The 514.5 nm line of an Ar^+ laser (Coherent, Innova model 305) was used as the excitation radiation, providing *ca.* 50 mW at the sample position. Samples were sealed in Kimax glass capillary tubes of 0.8 mm inner diameter. The system was calibrated against the crystalline silicon 521 cm^{-1} band. Under the above mentioned conditions, the error in wavenumbers was estimated to be less than 1 cm^{-1} and the resolution was better than 2 pixels of the CCD, *i.e.* 2 cm^{-1}.

2.4 Low resolution Raman spectroscopy

Low resolution spectra were recorded on a Bayspec Agility Raman spectrometer equipped with a 785 nm laser working at 300 mW. 10 mM Nb$_{10}$ samples were prepared by adding 25 mg of solid Nb$_{10}$ to the buffer solutions (1.5 ml, 0.1 M) with the pH already pre-adjusted using dropwise addition of [N(CH$_3$)$_4$]OH (1.0 M) in order to avoid pH shock. The pH value was recorded after the Nb$_{10}$ addition. The following buffers and pH were used: MES (pH 6.13), PIPES (pH 7.28), HEPES (pH 8.18), CHES (pH 9.05), CAPS (pH 10.08 and pH ∼ 11.12) and [N(CH$_3$)$_4$]OH (pH ∼ 12.80). The pH was measured with a Sigma-Aldrich micro pH combination electrode calibrated between pH 4.01 and 10.01. The alkaline error is likely to be very significant only for the 0.1 M [N(CH$_3$)$_4$]OH solution (pH 12.80). The solutions were pressed through 0.2 micrometer membrane filters which diminish, but do not eliminate, the Tyndall effect, as is typical. Spectra were collected after *ca.* four hours at 293 K. The speciation diagram in Fig. 3 was constructed assuming that the signal intensity of 10 mM Nb$_{10}$ was *ca.* 70 cps.

2.5 Computational details

All calculations were performed with Gaussian 09 rev B.[37] All structures were optimised using the PBE0 (PBE1PBE) exchange correlation functional and the def2-tzvp basis set, using an ultrafine grid and implicit water solvation using the polarizable continuum model.[38] Basis sets were obtained from the Basis Set Exchange.[39] Raman calculations were carried out at the same level of theory as the optimisations.

3. Results and discussion

3.1 NMR spectroscopy

Decavanadate and Nb$_{10}$ are isostructural and isoelectronic nanometre-sized polyoxometalate anions (Fig. 1). These relatively inflexible and structurally compact anions contain three types of metal sites: one site with four equivalent niobium (or vanadium) atoms above and below the major
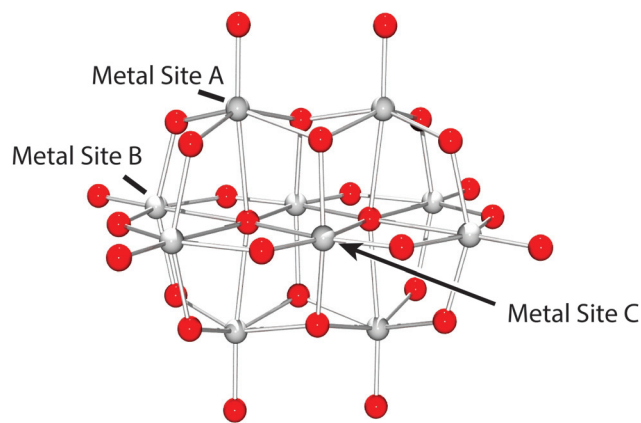

Fig. 1 Structure of the V$_{10}$ and the Nb$_{10}$ ions. The grey (light color) and red (dark color) spheres represent vanadium/niobium and oxygen atoms, respectively. The <Nb−O> bond lengths are 0.05−0.2 Å longer than the corresponding <V−O> bond lengths, making Nb$_{10}$ slightly larger than V$_{10}$.

equatorial plane (metal site A), one site with four equivalents in that plane (metal site B), and one site with two equivalents in both the major and minor equatorial planes (metal site C) (Fig. 1).

^{51}V-NMR spectroscopic studies demonstrated that, after acidification of the metavanadate solution from pH 6.7 to pH 4.0, we obtain a V$_{10}$ solution containing decameric vanadate species (Fig. 2). The identity was confirmed by the presence of

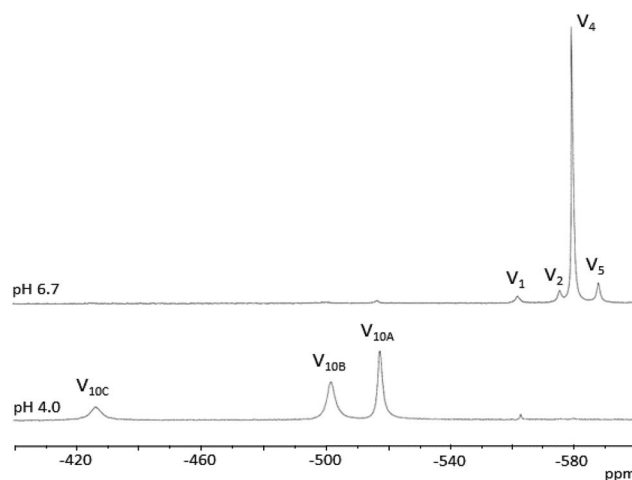**Fig. 2** ^{51}V NMR (105.2 MHz, 9.4 T) spectra, at ambient temperature of 50 mM (total vanadium) concentration of decavanadate (pH 4.0) (A) and metavanadate solutions (pH 6.7) (B). All spectra were acquired in the presence of 10% D$_2$O. V$_{10A}$, V$_{10B}$ and V$_{10C}$ represent signals of vanadium sites in V$_{10}$. The ^{51}V NMR V$_1$ signals correspond to the orthovanadate species namely, monomeric vanadate (VO$_4^{3-}$, HVO$_4^{2-}$ and H$_2$VO$_4^-$), whereas the metavanadate species includes dimeric V$_2$ (HV$_2$O$_7^{3-}$ and H$_2$V$_2$O$_7^{2-}$), regardless of the state of protonation, V$_4$ and V$_5$, that corresponds to cyclic tetrameric ([V$_4$O$_{12}$]$^{4-}$) and pentameric vanadate ([V$_5$O$_{15}$]$^{5-}$), respectively.

three NMR signals at −517, −501 and −426 ppm, respectively, corresponding to the three metal sites: V_{10A}, V_{10B} and V_{10C} (Fig. 2), in the expected intensity ratios. As can be observed by ^{51}V NMR, the solutions of 5 mM V_{10} (50 mM total vanadium, pH 4.0) contain mainly V_{10} species (Fig. 2). Conversely, in the NMR spectrum of a 50 mM metavanadate solution (pH 6.7), signals attributed to mono- (V_1), di- (V_2), tetra- (V_4) and penta-meric (V_5) species of vanadate can be observed, respectively, at −561 ppm, −575 ppm, −579 ppm and −587 ppm (Fig. 2), as previously described.[4] As expected, we observe that acidifica-tion of a colorless metavanadate solution turns the solution yellow/orange due to pH shock and metastable formation of the V_{10} ion, which dissociates slowly even at a pH where it is not ultimately stable. By 'pH shock' we mean that metastable species form upon addition of a drop of a base or acid, and these species are kinetically persistent. Upon acidification of 50 mM and higher vanadate concentrations it is possible to observe the solution becoming dark for a while at pH 5. This indicates that the species that forms are not thermo-dynamically stable at pH 5. Most likely it is due to pH shock. To the best of our knowledge, only VO^{2+} and $H_xV_{10}O_{28}^{(6−x)−}$ are coloured, so one of these species would be suggested to be formed. The latter would be formed at the pH near the pH of the acid added to the vanadate solutions and that would imply the reduction of vanadate species whereas the former due to vanadate oligomerization. The observation of the formation of these species would not be feasible or possible by NMR and/or Raman spectroscopy. However, kinetic studies using UV-Vis spectroscopy would be suitable to follow the formation and disappearance of these species.

The speciation diagram for aqueous solutions of vanadate shows that the V_{10} ion dominates between 2.5 and 5.8, to the point where it represents all of the total vanadate species at pH 3.0–5.0 (Fig. 3a). Similarly, the Nb_{10} ion is the dominant signal at 5.5 < pH < 9.90 and is detectable up to pH ∼ 10.8, whereas V_{10} slowly dissociates at most pH values and Nb_{10} converts quantitatively to the hexaniobate product at pH ∼ 11 (Fig. 3b). To date, there is no comprehensive speciation model for niobate aqueous solutions, as opposed to vanadate. However, ^{17}O NMR experiments have shown that the Nb_{10} species is stable for weeks between pH 5.5 and 7.5. Under higher pH conditions, the dissociation is detectable as a slow loss of signal from an internal oxygen in ^{17}O-enriched com-pounds.[30] The authors found the dissociation products to include the Nb_6 Lindqvist ion.[40] This dissociation is suspected to be reversible, based in part on isotope-transfer between the Nb_{10} and Nb_6 although the thermodynamics of the equili-brium remains unexplored.[40] Direct acidification of Nb_{10} in aqueous solution leads to the precipitation of a white powder referred to as 'niobic acid' in the literature. A dimer of the decaniobate ion, $[Nb_{20}O_{54}]^{8−}$, can be formed in dichloro-methane at low pH.[30] Little is known about the behaviour at very high pH (>14) but as salts of $[NbO_4]^{3−}$ are only known as insoluble solids, and $K_7H[Nb_6O_{19}]$ is synthesised in molten KOH,[36] it is unlikely that there is any polyoxoniobate chemistry beyond the Nb_6 ion in the alkaline direction.
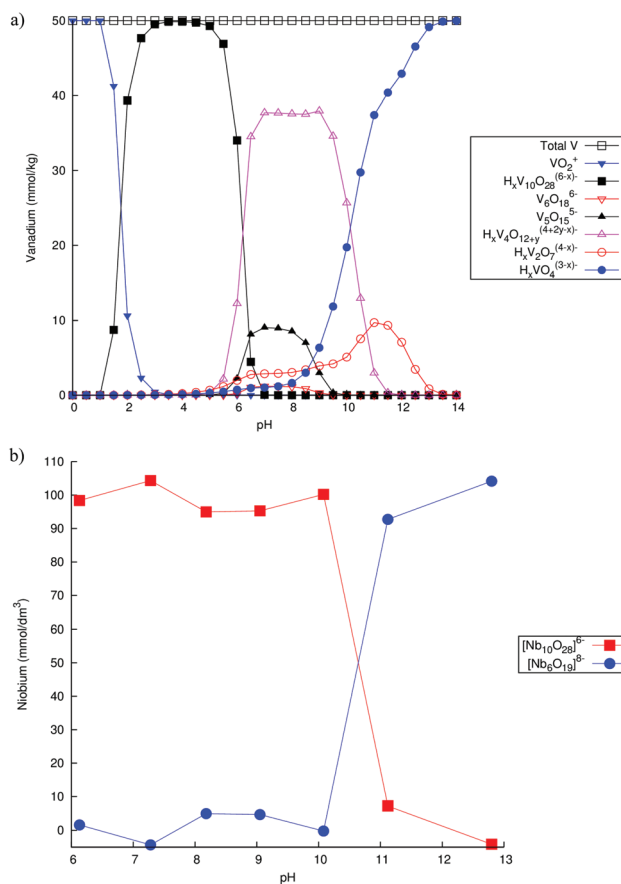

Fig. 3 (A) Speciation diagram based on ^{51}V-NMR, for an aqueous 50 millimolal (50 mmol $kg^{−1}$) solution of vanadium(v) at pH 0–14, showing the atomic concentration of vanadium i.e. the molecular con-centration of each species is multiplied by the number of vanadium atoms incorporated into it. The speciation at each pH was computed using Visual MINTEQ v3.0 [http://vminteq.lwr.kth.se/] in the presence of 1.0 M NaCl with a fixed 1.0 M ionic strength using the SIT model.[44] (B) Speciation diagram of niobates at 293 K at ca. 0.1 M ionic strength based on the current Raman spectrometric work. See the text for details as well as the ESI.†

3.2 Raman spectroscopy

We presently examine the stability of V_{10} species by Raman spectroscopy. A pH 4–12 range was chosen because it covers the biologically interesting range. On the other hand, the nio-bates condense by proton-induced charge neutralization under lower pH conditions whereas decavanadate persists under slightly lower pH conditions. Nevertheless, our focus was on the rich speciation chemistry at neutral pH and above. Fig. 4 depicts the Raman spectra of a 5 mM V_{10} solution in the 900–1100 $cm^{−1}$ region, for pH values ranging from 7.47 to 6.45. In this pH range, the signals are assignable to the VO symmetric stretching vibration of different oligomeric species. In particular, the band at 995 $cm^{−1}$ is due to the V_{10} species. This prevalence of V_{10} is in contrast with what is expected taking in consideration the speciation diagram for thermo-dynamically equilibrated solutions in this pH range, which predicts that the solution should not contain any appreciable
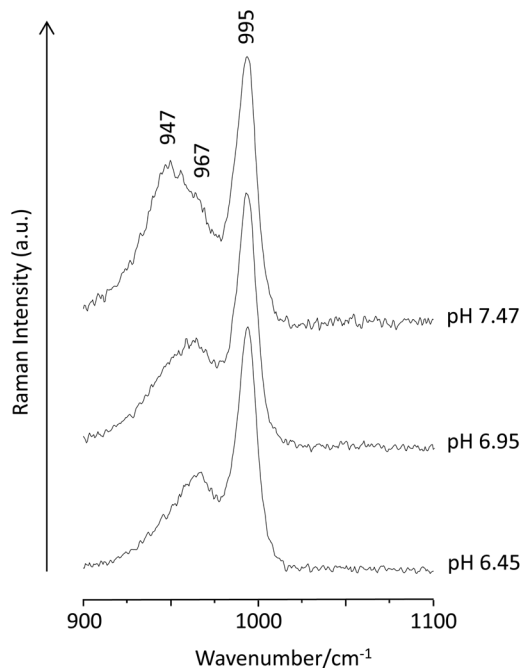
Fig. 4 Raman spectra of decavanadate solutions (50 mM total vanadium) from pH 6.45 to 7.47.

amount of V_{10}, but mainly V_4, with some V_5, V_2 and V_1. In fact, the spectra undergo a sequence of changes with pH: at pH 6.95 an additional band at 947 cm^{-1} begins to emerge and becomes completely distinguishable at pH 7.47 (Fig. 4). This signal clearly corresponds to another species, probably a tetrameric vanadate resulting from some V_{10} decomposition. This disparity is due to the solution being pH shocked and still under kinetic control.

The ^{51}V NMR studies showed that on acidification of vanadate solutions (pH 6.6), V_{10} appears together with the V_1, V_2 and V_4 which were already present in the vanadate solution at pH 6.8.[4] Raman bands ascribed to V_{10} are also observed at 315 and 593 cm^{-1}, in addition to the ones at 967 and around 995 cm^{-1} (Fig. 5). These V_{10} former bands are clearly visible in the Raman spectrum from 4.0 to pH 8.59 (Fig. 5). Conversely, at pH 8.97 V_{10} is no longer detectable, whereas the band at 947 cm^{-1} that began to emerge at pH 6.95 increasingly dominates the spectrum for higher pH values (Fig. 5). This signal was assigned in a previous study,[26] to the symmetric stretching vibration mode from V_4 and V_5 species, which agrees with the predicted speciation diagram in Fig. 1. At pH 9.52 a band, allocated to V_2 and HV_1 species, arises at 875 cm^{-1}. The band at 820 cm^{-1} assigned to the unprotonated V_1 species is only observed at a pH value close to 12.[29] Furthermore, after two weeks of incubation at 40 °C, similar spectra were obtained (not shown) for all the solutions described in Fig. 5.

In the Raman spectrum of decaniobate the bands at 936 and 270 cm^{-1} arise from the Nb_{10} ion (Fig. 6), with the band at 953 cm^{-1} ascribed to $[N(CH_3)_4]^+$. The 936 cm^{-1} signal, assigned to the NbO symmetric stretching vibration, appears
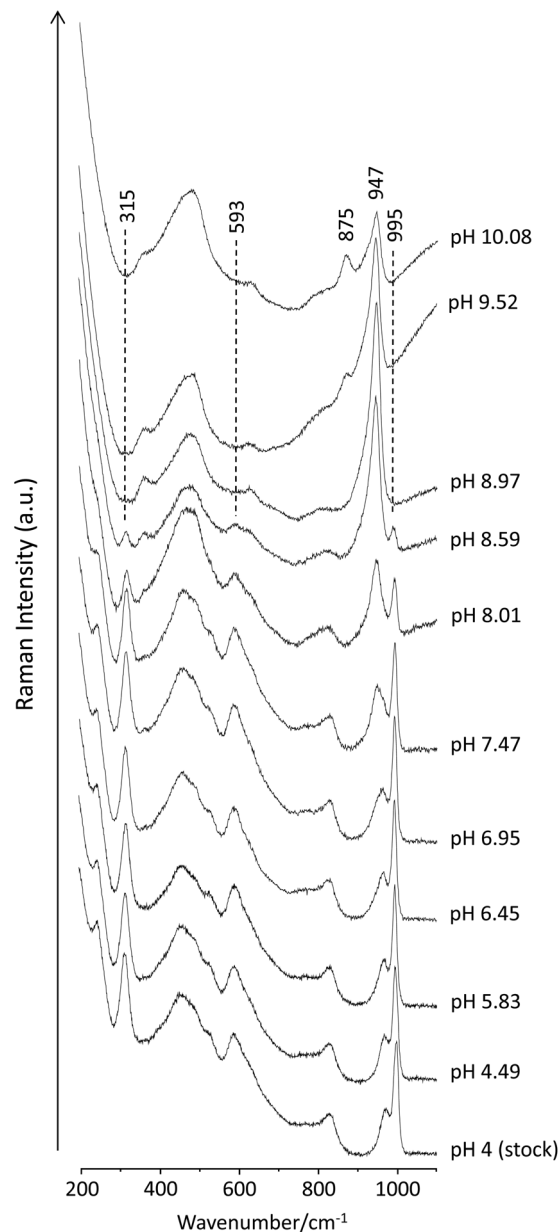

Fig. 5 Raman spectra (200 to 1100 cm^{-1}) of decavanadate solutions (50 mM total vanadium) from pH 4.00 to 10.08. The band between 400 and 500 cm^{-1} is due to the glass.

at a lower wavenumber than the corresponding one observed for the decavanadate, as expected assuming a similar force constant since niobium is a heavier element than vanadium. These bands are clearly observed up to pH 10.80 (Fig. 6), indicating the presence of Nb_{10} in the solution. No changes were observed on the spectra of the above solutions after two weeks of incubation at 40 °C, pointing out that the Nb_{10} solutions were stable even at higher alkaline pH values (Fig. 7).

The literature evidence for dissociation of the Nb_{10} at pH > 7.6 is from clear ^{17}O-NMR signal loss from oxygens in the center of the molecule.[40] The ^{17}O-NMR signal loss is quite slow and the authors suspected that there may be an equili-
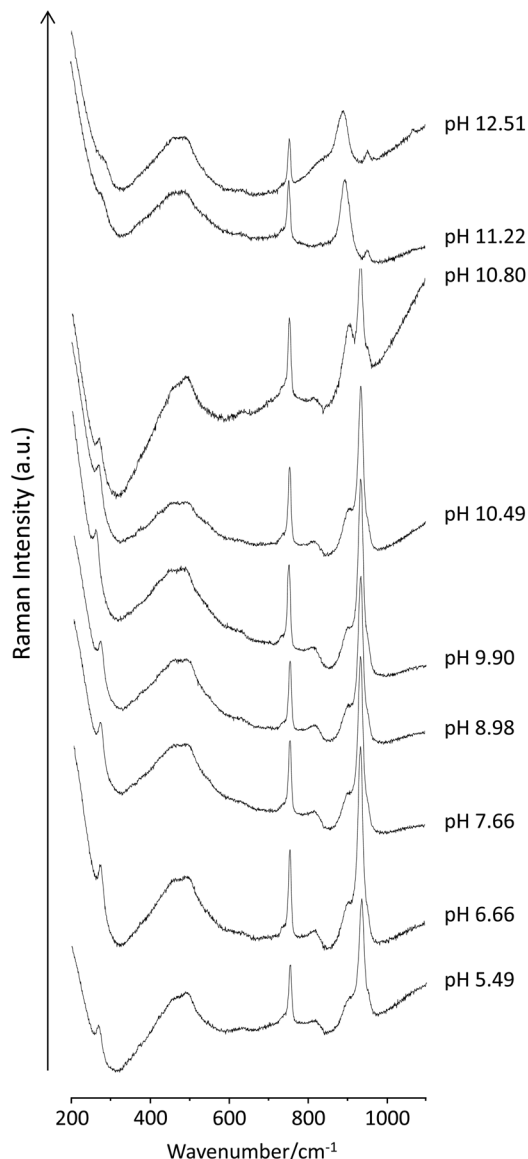
Fig. 6 Raman spectra (200 to 1100 cm^{-1}) of decaniobate solutions (50 mM total niobium) from pH 5.49 to 12.51.

brium between the Nb$_{10}$ and the Nb$_6$ dissociation product. The Raman spectra are consistent with Nb$_{10}$ being present in solution up to pH 10.80 [Fig. 3b]. Thus, at pH 10.49, a slight separation of bands is observed, and at pH 10.80 the formation of a band at 889 cm^{-1} is attributed to the presence of Nb$_6$ (Fig. 6). Also there is no difference in the Raman spectra at pH 11.22 and 12.51 (Fig. 6). Furthermore, Nb$_{10}$ species are kinetically stable and present in solution up to pH 9.90 for at least two weeks at 40 °C, even for the higher pH values analysed (Fig. S1†). In fact, there is no description in the literature of species in solution smaller than Nb$_6$, suggesting that this species is stable at very high pH, as we discussed above.

In an attempt to obtain a more quantitative view of the solution compositions, we collected additional data on a low-power, low-resolution instrument on samples prepared using

0.1 M biological buffers to avoid the influence of pH shock that might result from the addition of an acid or base to solutions of the niobates. As can be seen in Fig. 7, the results show that it is possible to collect quantitative solution composition data for niobates even in the presence of stabilising buffers.

The results broadly agree with previous data by Villa *et al.* based on the ^{17}O NMR spectra of ^{17}O-enriched Nb$_{10}$ acquired at 35 °C which showed that Nb$_{10}$, at concentrations of 0.6 M (total Nb), slowly dissociates to Nb$_6$ at and above pH 7.5, with the dissociation occurring increasingly rapidly with increasing pH and can be affected by solution composition.[30] The reaction has been observed to be at least partially reversible by the dissolution of Nb$_6$ in a borate buffer and subsequent analysis by ESI-MS after 24 hours at room temperature, a result that was confirmed by Klemperer *et al.*, who noted that the formation of Nb$_{10}$ from Nb$_6$ was favoured by increasing temperature.[41]

In either case, Raman spectra may here present a unique opportunity for the thermodynamic resolution of the equilibrium between Nb$_6$ and Nb$_{10}$, which would constitute the first example of quantitative speciation data for any polyoxoniobate species. It also does not escape our attention that a similar approach could be used to detail the relationship between [Ta$_6$O$_{19}$]$^{8-}$ and [Ta$_{10}$O$_{28}$]$^{6-}$, the latter being isolated only recently.[42]

3.3 Comparison between computed and observed spectra

The electronic-structure calculations predict features of the Raman spectra well, with a systematic over-estimation of the reciprocal wavenumber (Fig. 8). Experimentally, V$_{10}$ exhibits a strong band at 995 cm^{-1}, which is predicted computationally (Fig. 8d) to manifest at 1059 cm^{-1}, together with bands between 614 and 627 cm^{-1} and at 334 cm^{-1} which are experimentally found at 593 and 315 cm^{-1}, respectively. This tendency to over-estimate the wavenumber of the signal is persistent and well-known[43] with the signal from V$_4$ showing up at 947 cm^{-1}, but being predicted to occur at 1002 cm^{-1} (Fig. 8c). The most important point, however, is that the calculations capture the general trend of the signals shifting to a lower frequency with decreasing chain length, as well as the decavanadate species having two pronounced signals around 1000 cm^{-1} (Fig. 8d).

The qualitative and quantitative agreement is much better for the niobate species, with a predicted signal maximum at 957 cm^{-1} (Fig. 8f) for Nb$_{10}$ which was observed at 936 cm^{-1}. However, as the main signal for the Nb$_6$ occurs at 889 cm^{-1} but is expected at 858 cm^{-1}, the good numerical agreement for Nb$_{10}$ may be entirely fortuitous, which is unsurprising as the computations do not accurately account for hydrogen bonding and other factors that are known to influence the spectra (Fig. 8e and f).

The [N(CH$_3$)$_4$]$^+$ signals are expected at 817 and 1020 cm^{-1}, but exhibit at 755 and 953 cm^{-1}. The shapes and number of predicted signals agree well with experiment, lending some confidence in assignments for the observed signals. The main signal from the Nb$_{10}$ at 957 cm^{-1} (computed shift) is due to a symmetric concerted stretch of the terminal oxygen sites away from the molecular centre, as is the main signal from the Nb$_6$ ion at 858 cm^{-1}. The Nb$_6$ signals between 520 and 530 cm^{-1} are
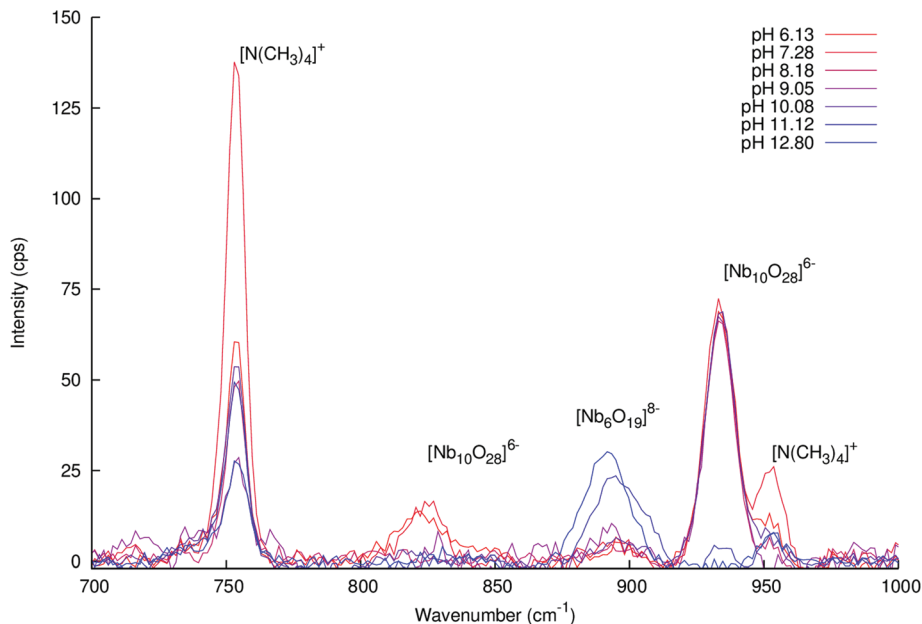
Fig. 7 Raman spectra of buffered solutions of Nb_{10} as a function of pH. Note that the $[N(CH_3)_4]^+$ concentration varies between solutions as $[N(CH_3)_4]OH$ was used to adjust the pH of the buffers.
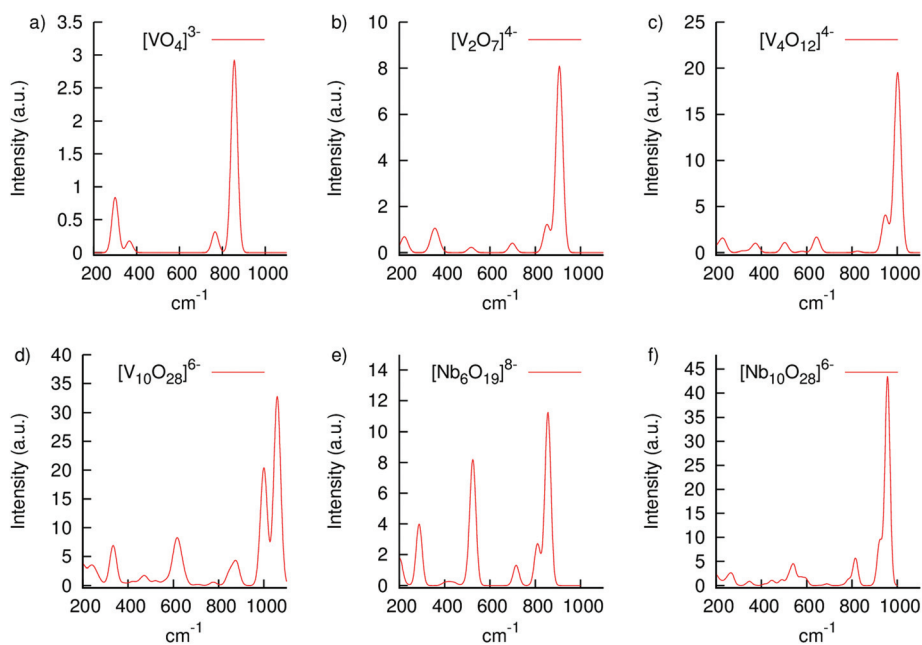

Fig. 8 Computed Raman spectra for select vanadate and niobate species. See the ESI† for numerical data.

due to movements of the central oxygen along an axis, and to the sets of μ_2-oxygens moving towards the molecular centre.

4. Conclusions

Raman spectra indicate that the V_{10} ion dominates in solution up to pH 6.45 and that this species remains detectable in solu-

tion until pH ~ 8.6. On the other hand, the Nb_{10} ion is the dominant signal at 5.5 < pH < 9.90 and is detectable up to pH ~ 10.8. Whereas V_{10} slowly dissociates at most pH values Nb_{10} converts quantitatively to the hexaniobate product at pH ~ 11 (Fig. 9). Nevertheless, Raman spectra point out that both V_{10} and Nb_{10} solutions are stable in solution for at least two weeks and moderate heat, in the sense that they do not precipitate a solid and that V_{10} and Nb_{10} are still detectable over a wide pH
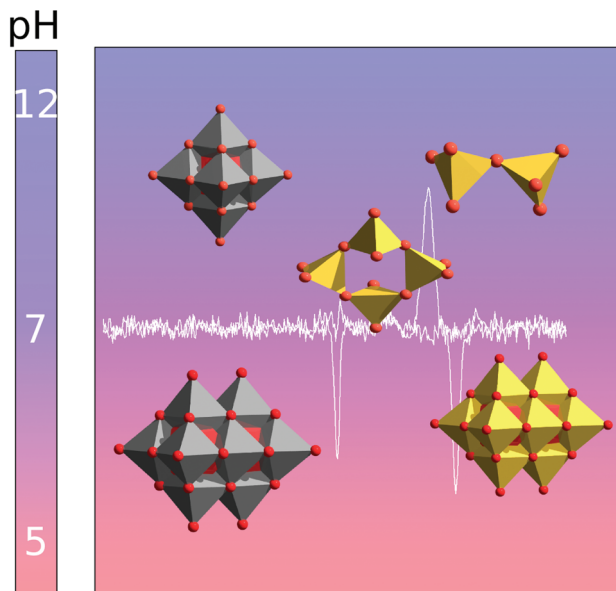
Fig. 9 V_{10} dissociates at most pH values into smaller tetrahedral vanadate oligomers such as V_4 and V_2, whereas Nb_{10} dissociates into Nb_6 under mildly or highly alkaline conditions.

range. Thus, Raman spectroscopy may be a potentially useful tool to characterize Nb_{10} and V_{10} species and their equilibrium with lower oligomers, which is extraordinarily difficult for niobate species because NMR is very difficult in the system. The vibrational properties, in contrast, can be established using electronic-structure methods *a priori* and used to assign the signals from putative minor aqueous species. These findings have important consequences for understanding the differences between decavanadate and decaniobate solution chemistry as well as its biological activities and pharmacological applications whenever a particular vanadate or niobate oligomer maybe desired and higher pH values are used.

Abbreviations

BMOV	Bis(maltolato)oxovanadium(IV)
CAPS	*N*-Cyclohexyl-3-aminopropanesulfonic acid
CHES	*N*-Cyclohexyl-2-aminoethanesulfonic acid
HEPES	4-(2-Hydroxyethyl)-1-piperazineethanesulfonic acid
MES	2-(*N*-Morpholino)ethanesulfonic acid
PIPES	Piperazine-*N*,*N*′-bis(2-ethanesulfonic acid)
Nb_{10}	Decaniobate ion $[Nb_{10}O_{28}]^{6-}$
Nb_6	Hexaniobate Lindqvist ion, $[Nb_6O_{19}]^{8-}$
SR	Sarcoplasmic reticulum
SR Ca^{2+}-ATPase	Calcium pump from sarcoplasmic reticulum
^{51}V-NMR	Vanadium-51 NMR
V_1	Monomeric vanadate, $[VO_4]^{3-}$
V_2	Dimeric vanadate, $[V_2O_7]^{4-}$
V_4	Tetrameric vanadate, $[V_4O_{12}]^{4-}$ and $[V_4O_{13}]^{6-}$
V_5	Pentameric vanadate, $[V_5O_{15}]^{5-}$
V_{10}	Decavanadate ion, $[V_{10}O_{28}]^{6-}$

References

1 J. T. Rhule, C. L. Hill and D. A. Judd, *Chem. Rev.*, 1998, **98**, 327–357.
2 T. Yamase, *J. Mater. Chem.*, 2005, **15**, 4773–4782.
3 M. Aureliano, *Oxid. Med. Cell. Longevity*, 2016, **2016**, 6103457, 8 pages.
4 M. Aureliano and D. C. Crans, *J. Inorg. Biochem.*, 2009, **103**, 536–546.
5 M. Aureliano, *Dalton Trans.*, 2009, 9093–9100.
6 M. Aureliano, *World J. Biol. Chem.*, 2011, **2**, 215–238.
7 S. Ramos, J. J. G. Moura and M. Aureliano, *Metallomics*, 2012, **4**, 16–22.
8 M. Aureliano, G. Fraqueza and C. A. Ohlin, *Dalton Trans.*, 2013, **42**, 11770–11777.
9 M. Aureliano, *Inorg. Chim. Acta*, 2014, **420**, 4–7.
10 M. Aureliano and C. A. Ohlin, *J. Inorg. Biochem.*, 2014, **137**, 123–130.
11 N. Samart, J. Saeger, K. J. Haller, M. Aureliano and D. C. Crans, *J. Mol. Eng. Mater.*, 2014, **2**, 1440007.
12 L. Yan-Tuan, Z. Chun-Yuan, W. Zhi-Yong, M. Jiang and C.-W. Yan, *Transition Met. Chem.*, 2010, **35**, 597–603.
13 F. Zhai, X. Wang, D. Li, H. Zhang, R. Li and L. Song, *Biomed. Pharmacother.*, 2009, **63**, 51–55.
14 X. Niu, R. Xiao, N. Wang, Z. Wang, Y. Zhang, Q. Xia and X. Yang, *Curr. Top. Med. Chem.*, 2016, **16**, 811–822.
15 V. Dimitrova, K. Zhetcheva and L. P. Pavlova, *J. Chem.*, 2011, **35**, 215–223.
16 R. Raza, A. Matin, S. Sarwar, M. Barsukova-Stuckart, M. Ibrahim, U. Kortz and J. Iqbal, *Dalton Trans.*, 2012, **41**, 14329–14336.
17 A. Zorzano, M. Palacin, L. Marti and S. Garcia-Vicente, *J. Inorg. Biochem.*, 2009, **103**, 559–566.
18 M. J. Pereira, E. Carvalho, J. W. Eriksson, D. C. Crans and M. Aureliano, *J. Inorg. Biochem.*, 2009, **103**, 1687–1692.
19 G. Borges, P. Mendonça, N. Joaquim, M. Aureliano and J. M. Coucelo, *Arch. Environ. Contam. Toxicol.*, 2003, **45**, 415–422.
20 X. Chen, S. Yan, H. Wang, Z. Hu, X. Wang and M. Huo, *Carbohydr. Polym.*, 2015, **117**, 673–680.
21 L. Mohapatra and K. M. Parida, *Phys. Chem. Chem. Phys.*, 2014, **16**, 16985–16996.
22 A. Bijelic and A. Rompel, *Coord. Chem. Rev.*, 2015, **299**, 22–38.

23 L. Pettersson, I. Andersson and A. Gorzsás, *Coord. Chem. Rev.*, 2003, **237**(1–2), 77–87.

24 A. Gorzsás, I. Andersson and L. Pettersson, *J. Inorg. Biochem.*, 2009, **103**, 517–526.

25 S. Ramos, M. Manuel, T. Tiago, R. O. Duarte, J. Martins, C. Gutiérrez-Merino, J. J. G. Moura and M. Aureliano, *J. Inorg. Biochem.*, 2006, **100**, 1734–1743.

26 T. Tiago, M. Aureliano and C. Gutierrez-Merino, *Biochemistry*, 2004, **43**, 5551–5561.

27 G. Fraqueza, L. A. E. Batista de Carvalho, M. P. M. Marques, L. Maia, C. A. Ohlin, W. H. Casey and M. Aureliano, *Dalton Trans.*, 2012, **41**, 12749–12758.

28 G. Fraqueza, C. A. Ohlin, W. H. Casey and M. Aureliano, *J. Inorg. Biochem.*, 2012, **107**, 82–89.

29 A. Amado, M. Aureliano, P. J. Ribeiro-Claro and J. Teixeira-Dias, *J. Raman Spectrosc.*, 1993, **24**, 669–703.

30 E. M. Villa, C. A. Ohlin, E. Balogh, T. M. Anderson, M. D. Nyman and W. H. Casey, *Angew. Chem., Int. Ed.*, 2008, **47**, 4844–4846.

31 R. S. Tobias, *Can. J. Chem.*, 1965, **43**, 1222–1225.

32 W. P. Griffith and T. D. Wickins, *J. Chem. Soc. A*, 1966, 1087–1090.

33 A. Goiffon and B. Spinner, *Rev. Chim. Miner.*, 1974, **11**, 262–268.

34 J.-M. Jehng and I. E. Wachs, *Chem. Mater.*, 1991, **3**, 100–107.

35 C. A. Ohlin, E. M. Villa and W. H. Casey, *Inorg. Chim. Acta*, 2009, **362**, 1391–1392.

36 Y. Liu, S.-X. Guo, L. Ding, C. A. Ohlin, A. M. Bond and J. Zhang, *ACS Appl. Mater. Interfaces*, 2015, **7**, 16632–16644.

37 M. J. Frisch, *et al.*, *Gaussian 09*, Gaussian, Inc., Wallingford, CT, USA, 2009.

38 J. Tomasi, B. Mennucci and R. Cammi, *Chem. Rev.*, 2005, **105**, 2999–3094.

39 K. L. Schuchardt, B. T. Didier, T. Elsethagen, L. Sun, V. Gurumoorthi, J. Chase, J. Li and T. L. Windus, *J. Chem. Inf. Model.*, 2007, **47**, 1045–1052.

40 C. A. Ohlin, E. M. Villa, J. C. Fettinger and W. H. Casey, *Angew. Chem., Int. Ed.*, 2008, **47**, 8251–8254.

41 W. G. Klemperer and K. A. Marek, *Eur. J. Inorg. Chem.*, 2013, 1762–1771.

42 M. Matsumoto, Y. Ozawa, A. Yagasaki and Y. Zhe, *Inorg. Chem.*, 2013, **52**, 7825–7827.

43 M. K. Kershawani, B. Brauer and J. M. L. Martin, *J. Phys. Chem.*, 2015, **119**, 1701–1714.

44 I. Grenthe, A. V. Plyasunov and K. Spahiu, in *Modelling in aquatic chemistry*, ed. I. Grenthe and I. Puigdomenech, OECD Nuclear Energy Agency, Paris, 1997, ch. IX, pp. 325–426.